Electronic Supplementary Material (ESI) for Dalton Transactions.

SUPPORTING INFORMATION

Unexpected formation of a fused double cycle trinuclear gold(I) complex supported by *ortho*-phenyl metallated aryl-diphosphine ligands and strong aurophilic interactions

Csaba Jobbágy,[a] Péter Baranyai,[a] Pál Szabó,[b] Tamás Holczbauer,[c] Barbara Rácz,[a] Liang Li,[d] Pance Naumov*[d] and Andrea Deák*[a]

[a]Hungarian Academy of Sciences, MTA TTK SZKI,
“Lendület” Supramolecular Chemistry Research Group,
1117 Budapest, Magyar Tudósok körútja 2, Hungary;
E-mail: deak.andrea@ttk.mta.hu

[b]Hungarian Academy of Sciences, MTA TTK SZKI,
MS Metabolomics Research Group,
1117 Budapest, Magyar Tudósok körútja 2, Hungary;

[c]Hungarian Academy of Sciences, MTA TTK SZKI,
Chemical Crystallography Research Group,
1117 Budapest, Magyar Tudósok körútja 2, Hungary;

[d]New York University Abu Dhabi, P.O. Box 129188,
Abu Dhabi, United Arab Emirates;
E-mail: pance.naumov@nyu.edu

Experimental Section

General Procedures and Physical Measurements

All chemicals and solvents used for the syntheses were of reagent grade. The solvents for synthesis were used without further purification. All manipulations were performed in air.

The exact mass was measured in a Waters QTOF Premier instrument (Waters, Milford, MA, USA) equipped with electrospray ionization source (Waters, Milford, MA, USA) used in the positive ion mode. The mass spectrum was recorded using the software MassLynx 4.1 (Waters, Milford, MA, USA) in the mass range 1000–2000 *m/z*. Infrared spectrum was recorded in the 400 to 4000 cm^{-1} spectral range on a Varian 2000 FT-IR spectrometer equipped with Golden Gate single reflection diamond ATR (Specac Ltd.).

Pyrolysis–gas chromatography/mass spectrometry (Py–GC/MS) measurements were carried out in a CDS Pyroprobe 2000 equipped with a platinum coil and quartz sample tube. About 0.6 mg sample was heated at 200°C for 20 s in a quartz tube using helium as a carrier gas. The pyrolyzer was coupled to an Agilent 6890/5973 GC/MS instrument, using Agilent DB-1701 capillary column (30 m × 0.25 mm i.d., 0.25 μm film thickness). The pyrolysis interface was heated to 180°C. The mass spectrometer operated at 70 eV in the EI mode, *m/z* : 14-500 were scanned.

Mass spectrometric measurements were performed on a Sciex QTRAP 6500 tandem mass spectrometer (Sciex, MA, USA) equipped with TurboV ion source. Samples were dissolved in dichloromethane and diluted with acetonitrile prior to measurements. This diluted sample was injected directly into the mobile phase (acetonitrile). The mobile phase was delivered by a Perkin Elmer S200 micro LC pump with a flow of 200 µL/min. MS spectra were recorded in positive ion detection mode. Mass range was 400-2000 Da. MS spectra were recorded both in Q1 and ion trap (EMS) mode. Isotope patterns were identified in enhanced resolution (ER) mode. Tandem mass spectrometric measurements were acquired in ion trap mode: enhanced product ion (EPI) using collision energy of 45 eV. Source conditions were: curtain gas: 35 psi, spray voltage: 5000 V, temperature: 350°C, nebulizer gas: 30 psi, drying gas: 30 psi, declustering potential: 135 V. The HRMS studies was performed with a Waters QTOF Premier instrument (Waters, Milford, MA, USA) equipped with electrospray ionization source (Waters, Milford, MA, USA) used in the positive ion mode. Mass spectra were recorded using the software MassLynx 4.1 (Waters, Milford, MA, USA) in the mass range 1000–2000 *m/z*. NMR experiments were carried out on Varian Inova (400 MHz for ^{1}H) spectrometer using a switchable broadband X{^{1}H}, and an inverse detection triple tuneable pfg 5mm ^{1}H^{13}C{X} probe (X = ^{31}P) respectively. Samples were placed into 5 mm NMR tube and the measuring temperature was 25 °C. ^{1}H chemical shifts are referenced to the residual solvent signal (CD_2Cl_2: 5.32 ppm). ^{31}P shifts are given relative to the external reference 85% H_3PO_4. Deuterated (99.98 atom%) solvent was purchased from Merck® GmBH, Germany. ^{1}H spectra were recorded with 16 seconds, while the ^{31}P spectra with 12 seconds relaxation delay and WALTZ-16 proton decoupling.

The UV–VIS spectra in solution phase were measured on an Agilent 8452A photodiode array spectrometer. Steady state and time-resolved luminescence measurements were carried out on an Edinburgh Instrument FLSP920 spectrofluorimeter. Spectral corrections were applied using excitation and emission correction functions of the instrument. Longpass filters were used to exclude the scattered excitation light. The solid-state luminescence measurements at low-temperature (77 K) were recorded in a quartz capillary tube immersed in liquid nitrogen. The excitation light source was a µF900H xenon flashlamp (pulse duration: 2 µs at FWHM) for the luminescent lifetime measurements. Solutions were deoxygenated by bubbling high purity N_2 for 15 minutes before lifetime measurements.

Movie S1 showing the hopping off the stage of crystal **1** upon heating to 220 °C was recorded with a LINKAM Imaging Station microscope equipped with Nikon DS-Fi1c digital camera.
Movie S2 showing the heating of crystal **1** in 250 °C silicone oil was recorded with a Leica M80 microscope equipped with Leica MC120 HD digital camera.
SEM image of **1** was taken on a FEI Quanta FEG 450 Scanning Electron Microscope.

Synthesis and characterisation

The starting $[Au_2(xantphos)_2](NO_3)_2$ (**1**) complex was prepared according to a published procedure.[1] Complex **2** and its characterization was reported by Lagunas and co-workers.[2]

1 (240 mg, 0.04 mmol) was heated in a thermoblock at 180 °C for 40 minutes. To the as-obtained brownish powder toluene (20 mL) was added and the resulting suspension was stirred for 20 minutes, then filtered off. Subsequently, the brownish residue was dissolved in dichloromethane toluene mixture (1:1, 20 mL) and filtered through Celite. The as-resulting clear yellow solution was placed in a thermoblock at 50 °C. Beautifully formed colourless crystals of **2** and yellow crystals of **3** were obtained over three days (Figure S1). The crystals were filtered off and washed with cold toluene. The yellow crystals of **3** were separated manually (Figure S2).

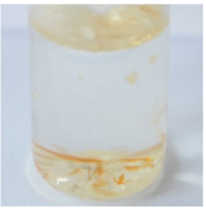

Fig. S1 Bulky colourless crystals (**2**) and tiny yellow plates (**3**) obtained upon crystallization of the thermolysate of **1** from dichloromethane and toluene mixture.

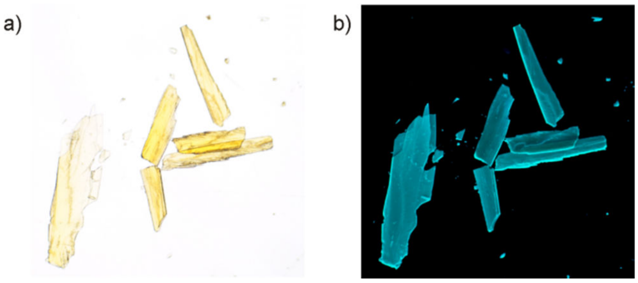

Fig. S2 Microscopic images of crystals of **3** under a) ambient light and b) UV light (365 nm).

Compound **3**: IR data: 3647 (w), 3381 (w, br), 3052 (m), 2955 (m), 1607 (w), 1586 (w), 1480 (w), 1436 (m), 1403 (s), 1337 (s), 1227 (s), 1180 (m), 1099 (m), 1028 (w), 998 (w), 876 (w), 781 (w), 743 (m), 719 (w), 690 (m), 604 (w), 588 (w), 537 (w), 516 (w); HRMS–ESI (*m/z*): $[Au_3(L')_2]^+$ calcd for $C_{78}H_{62}Au_3O_2P_4$, 1745.270; found, 1745.277 (Figure S3).

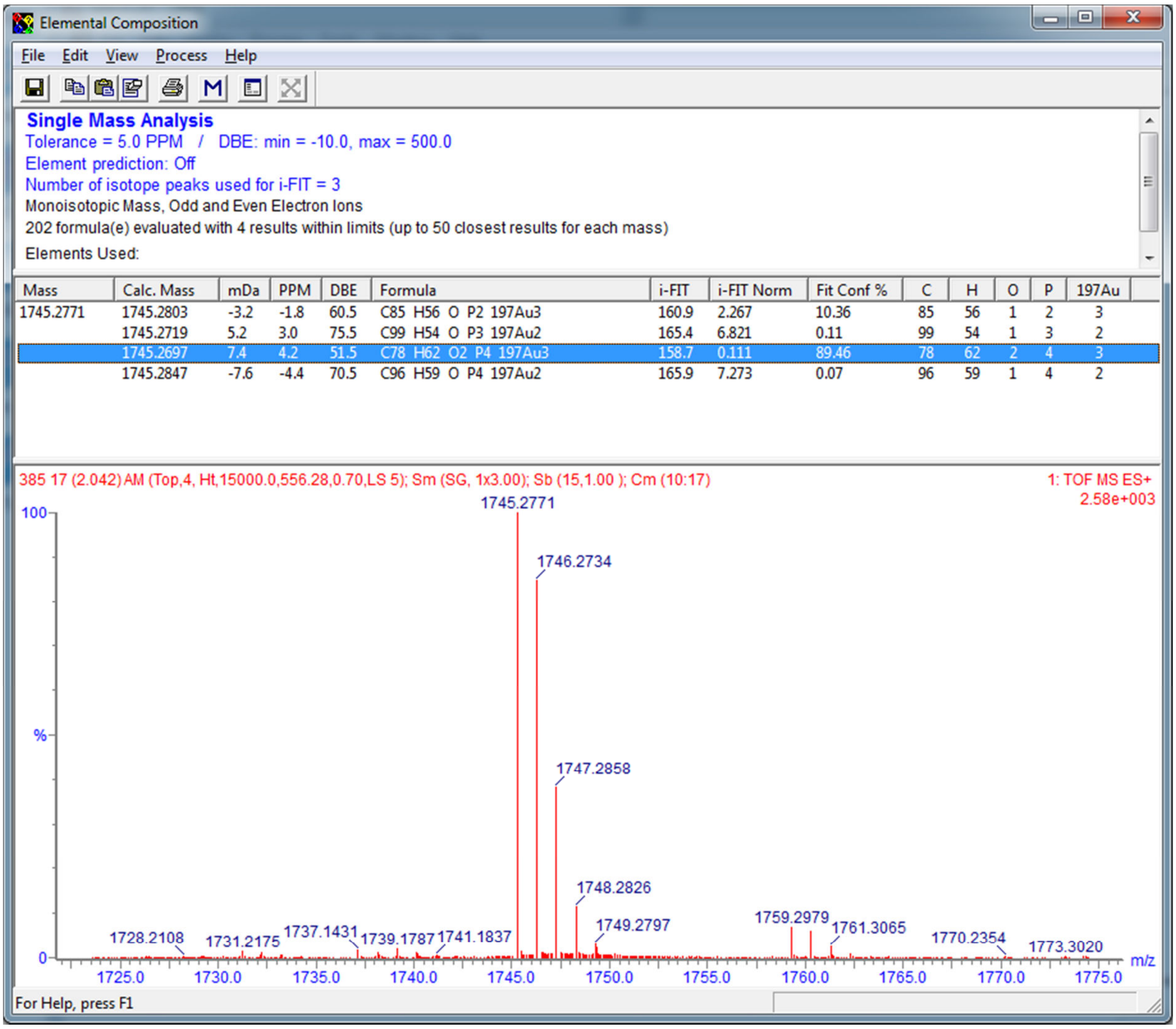

Single Mass Analysis
Tolerance = 5.0 PPM / DBE: min = -10.0, max = 500.0
Element prediction: Off
Number of isotope peaks used for i-FIT = 3
Monoisotopic Mass, Odd and Even Electron Ions
202 formula(e) evaluated with 4 results within limits (up to 50 closest results for each mass)
Elements Used:

Mass	Calc. Mass	mDa	PPM	DBE	Formula	i-FIT	i-FIT Norm	Fit Conf %	C	H	O	P	197Au
1745.2771	1745.2803	-3.2	-1.8	60.5	C85 H56 O P2 197Au3	160.9	2.267	10.36	85	56	1	2	3
	1745.2719	5.2	3.0	75.5	C99 H54 O P3 197Au2	165.4	6.821	0.11	99	54	1	3	2
	1745.2697	7.4	4.2	51.5	C78 H62 O2 P4 197Au3	158.7	0.111	89.46	78	62	2	4	3
	1745.2847	-7.6	-4.4	70.5	C96 H59 O P4 197Au2	165.9	7.273	0.07	96	59	1	4	2

385 17 (2.042) AM (Top,4, Ht,15000.0,556.28,0.70,LS 5); Sm (SG, 1x3.00); Sb (15,1.00); Cm (10:17)
1: TOF MS ES+
2.58e+003

Fig. S3 HRMS-ESI spectra of $[Au_3(L')_2]^+$.

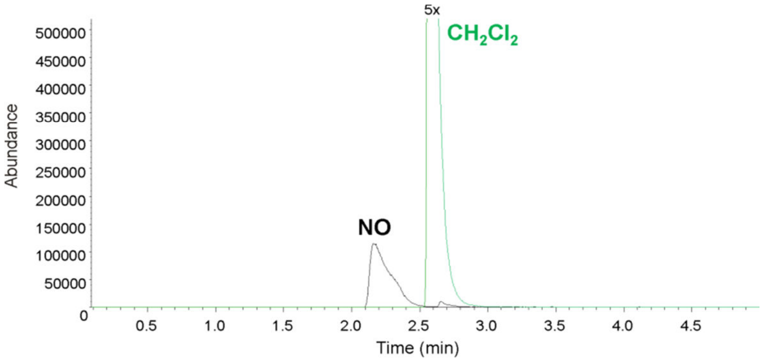

Fig. S4 Pyrolysis-GC/MS ion-chromatographic peaks of NO (*m/z*: 30) and CH_2Cl_2 (*m/z*: 84) evolved from **1** at 200°C pyrolysis temperature.

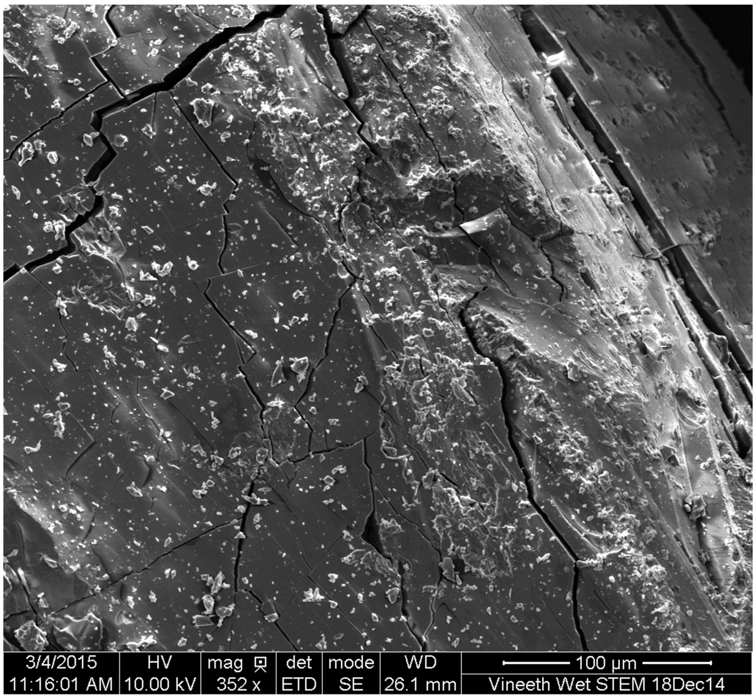

Fig. S5 Scanning Electron Microscopy image of crystal **1** after heated up to 250 °C.

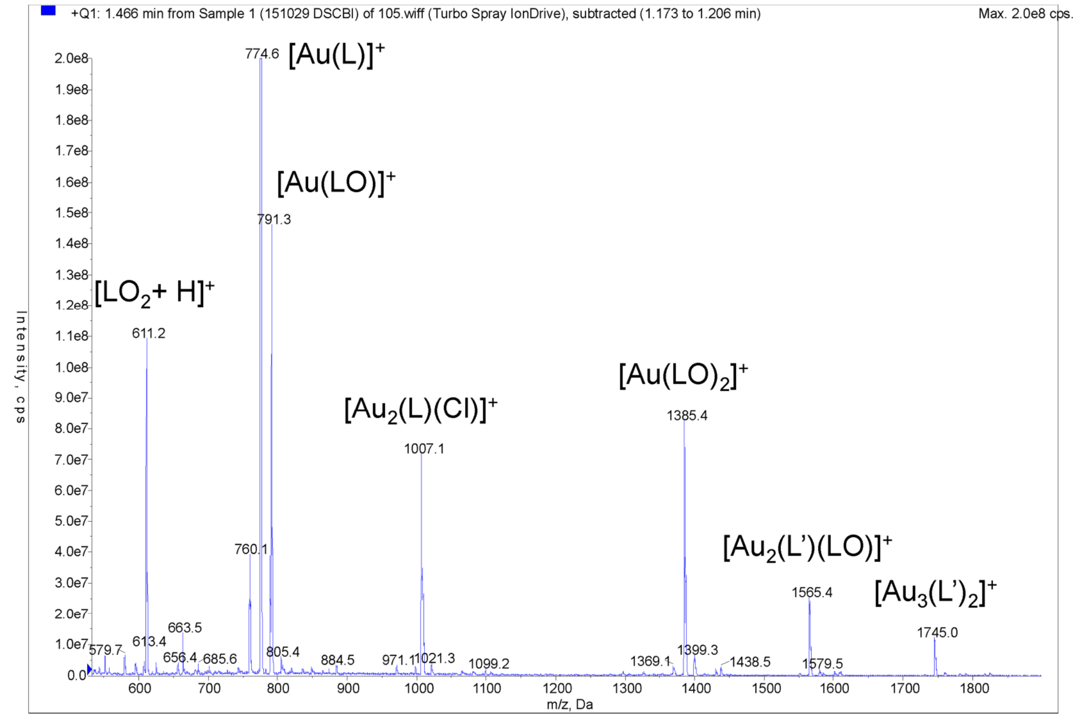

Fig. S6 A representative ESI(+)-MS spectrum of the brownish thermolysate of **1** in dichloromethane.

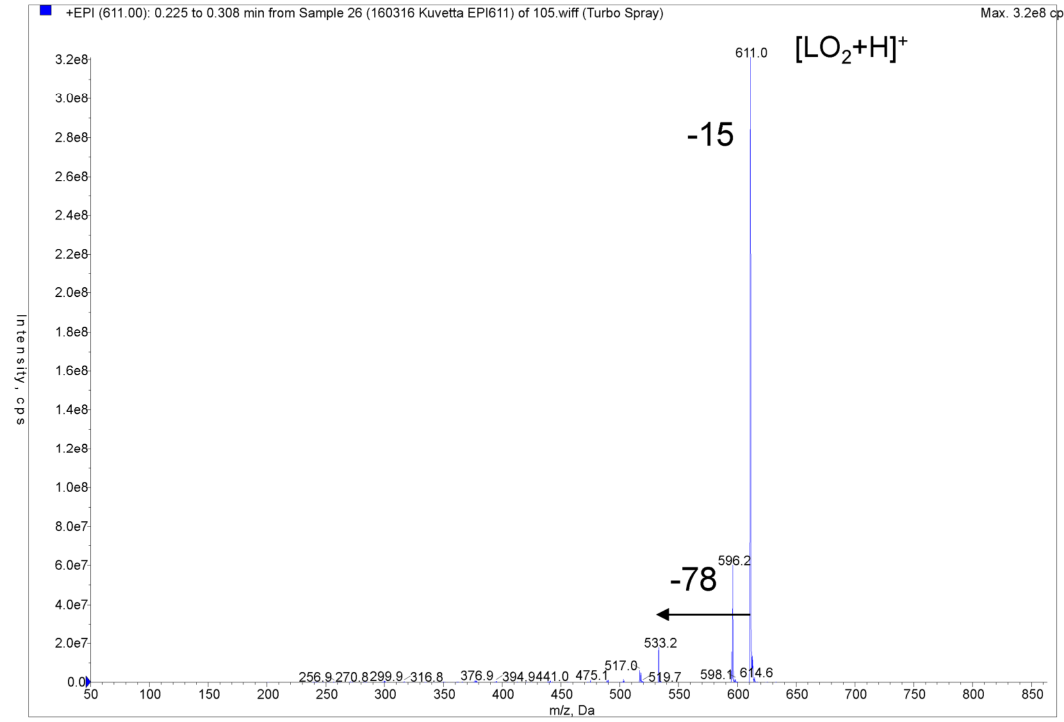

Fig. S7 ESI-MS/MS spectrum of $[LO_2 + 1H]^+$.

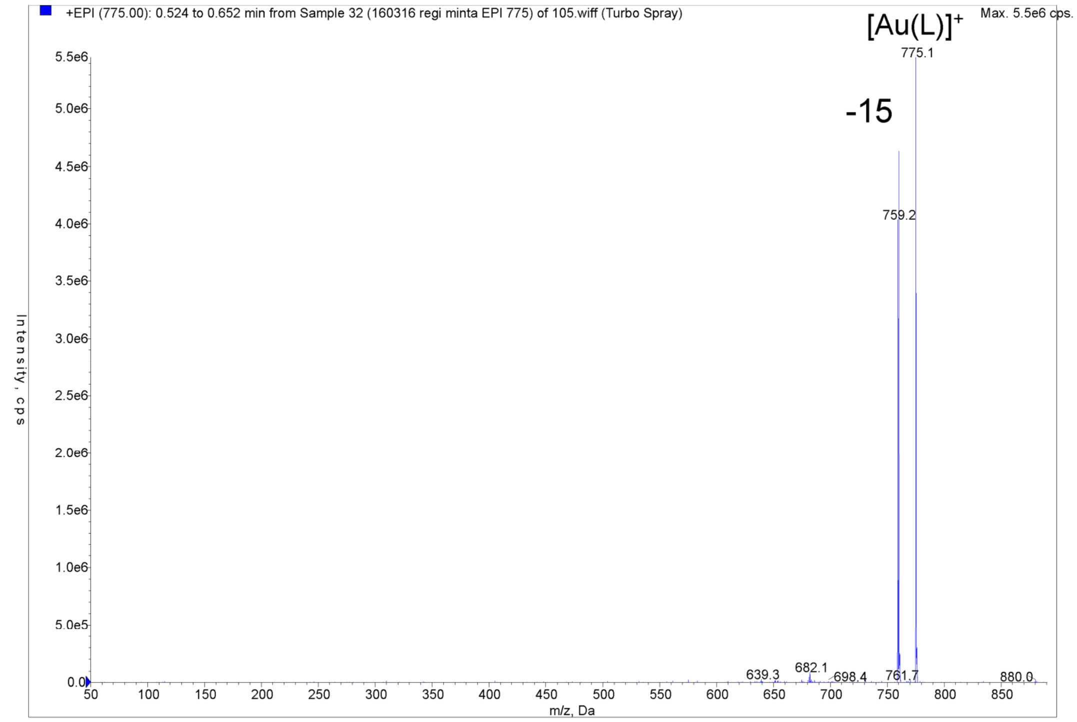

Fig. S8 ESI-MS/MS spectrum of [Au(L)]$^+$.

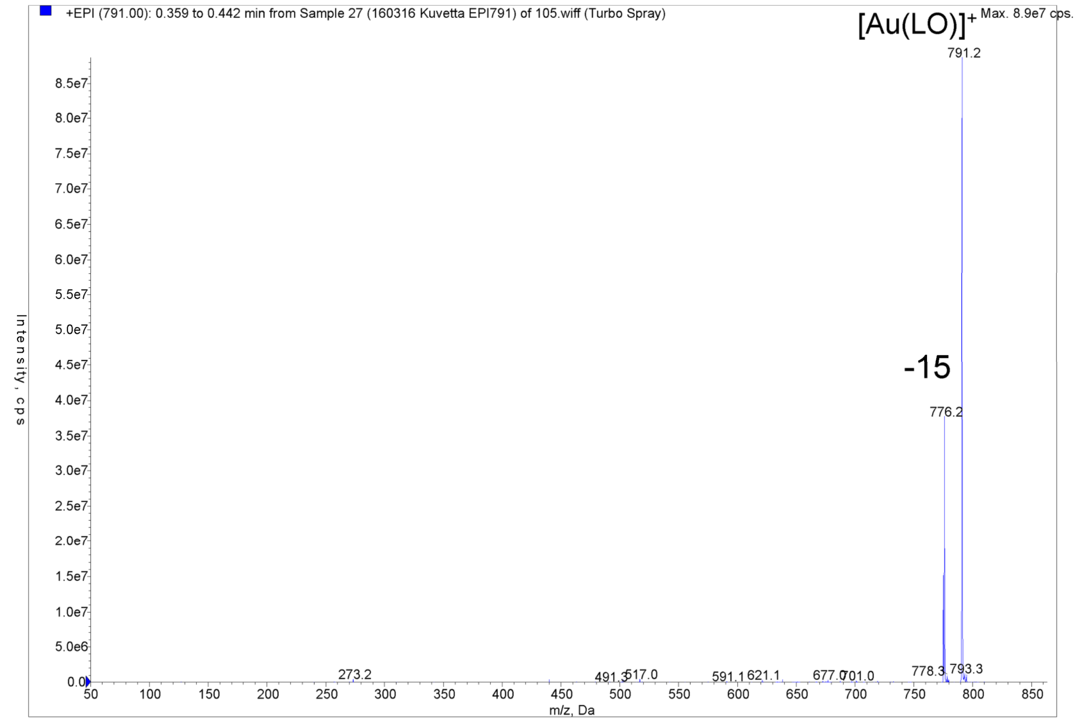

Fig. S9 ESI-MS/MS spectrum of [Au(LO)]$^+$.

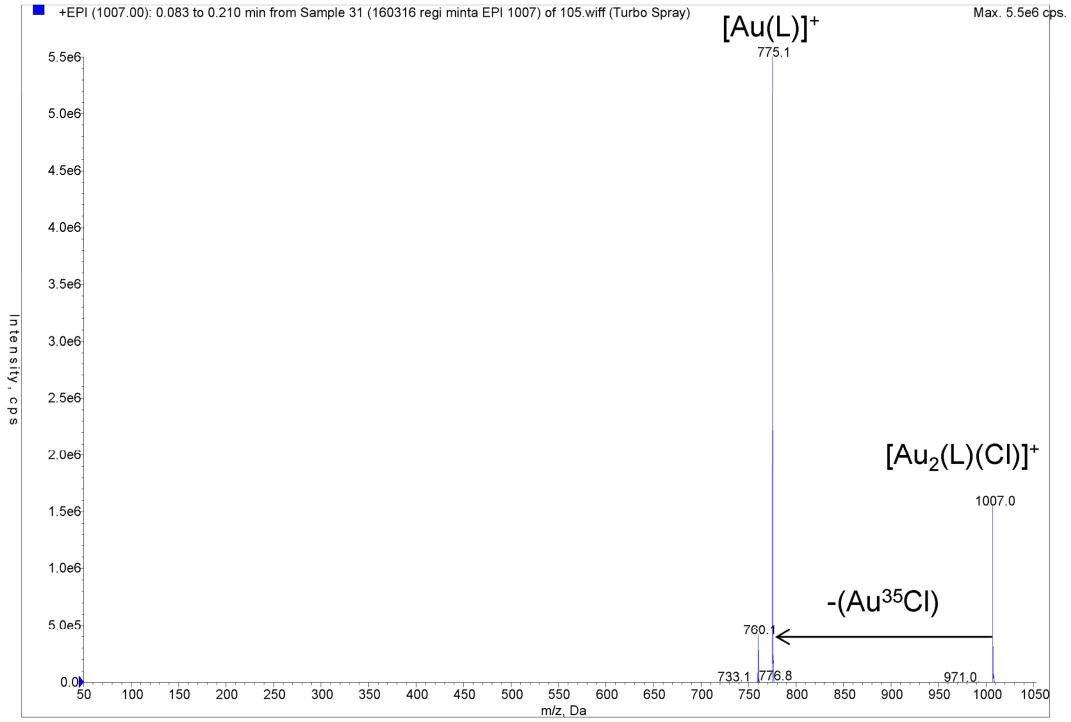

Fig. S10 ESI-MS/MS spectrum of $[Au_2(L)(Cl)]^+$.

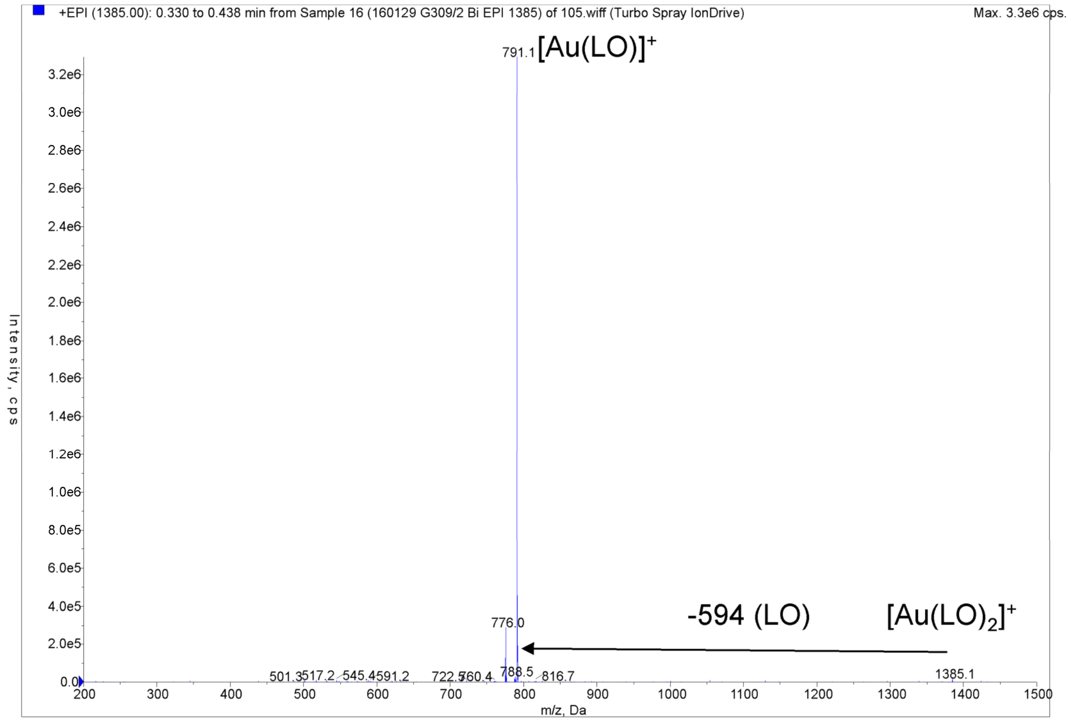

Fig. S11 ESI-MS/MS spectrum of $[Au(LO)_2]^+$.

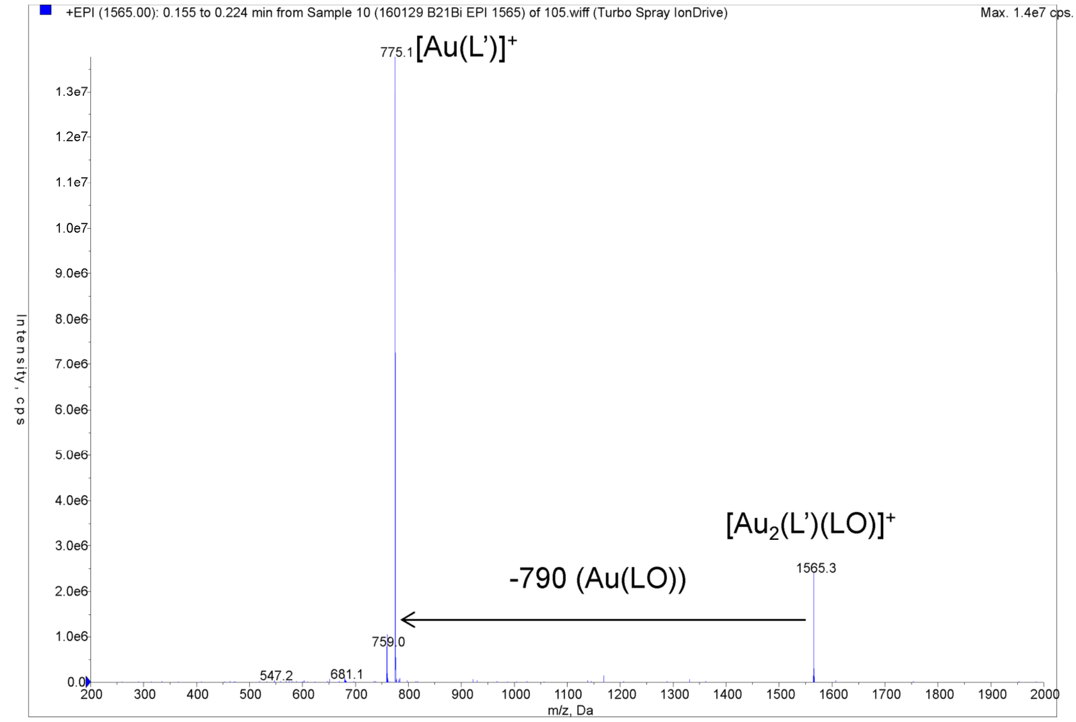

Fig. S12 ESI-MS/MS spectrum of $[Au_2(L')(LO)]^+$.

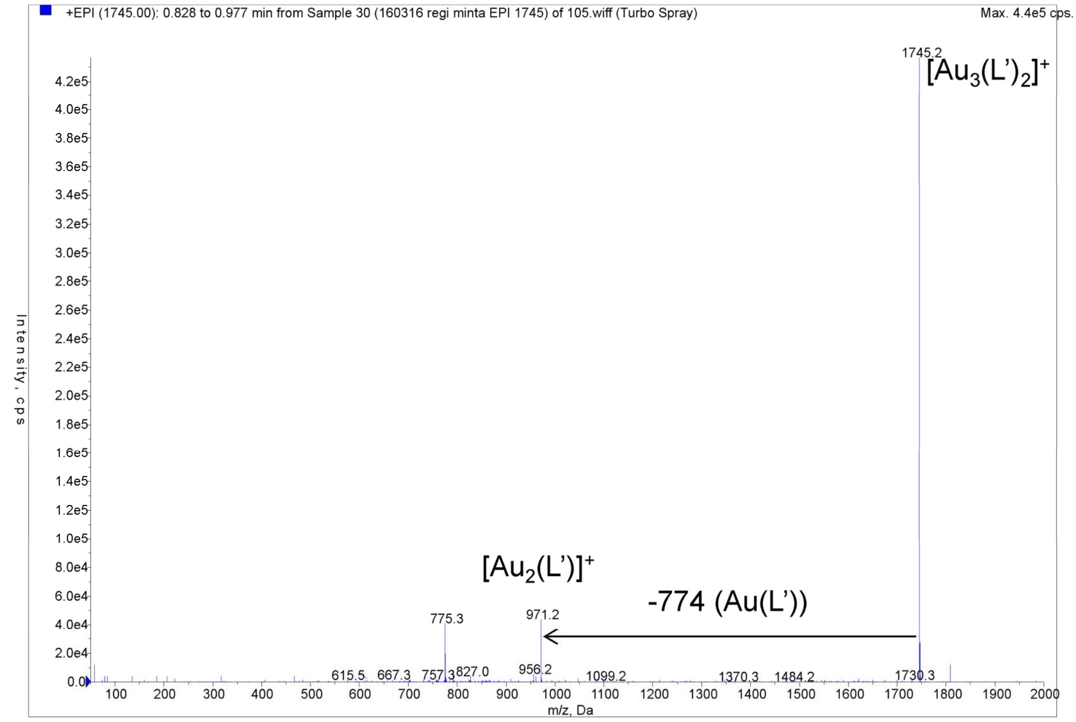

Fig. S13 ESI-MS/MS spectrum of $[Au_3(L')_2]^+$.

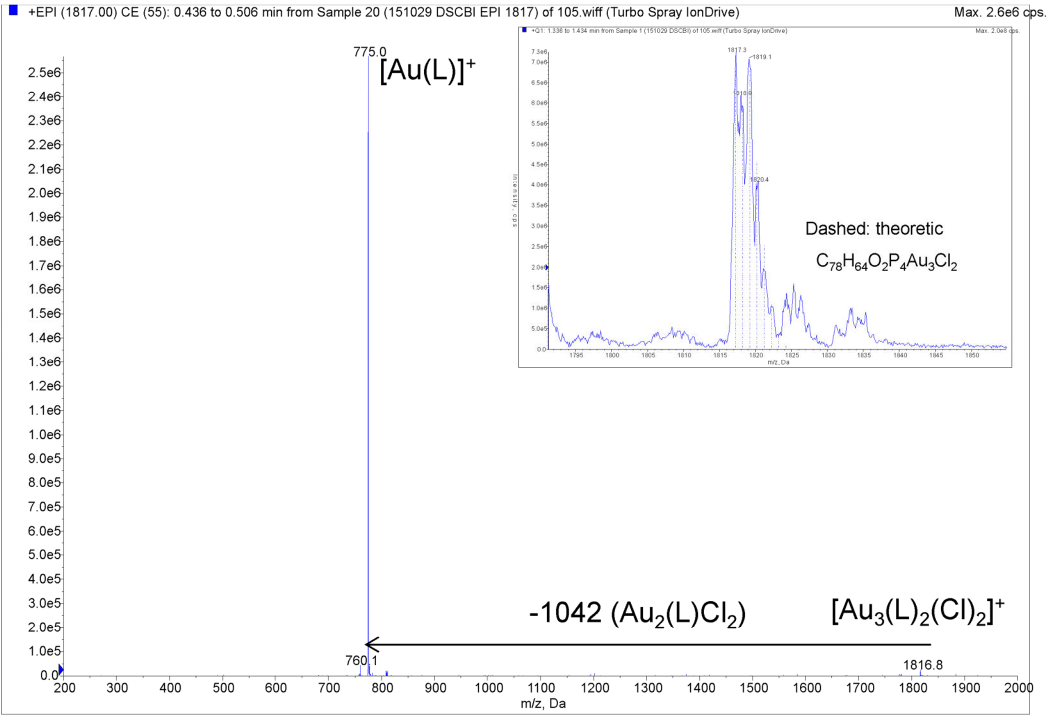

Fig. S14 ESI-MS/MS spectrum of $[Au_3(L)_2(Cl)_2]^+$. Inset: observed and theoretical isotopic mass distribution for $[Au_3(L)_2(Cl)_2]^+$.

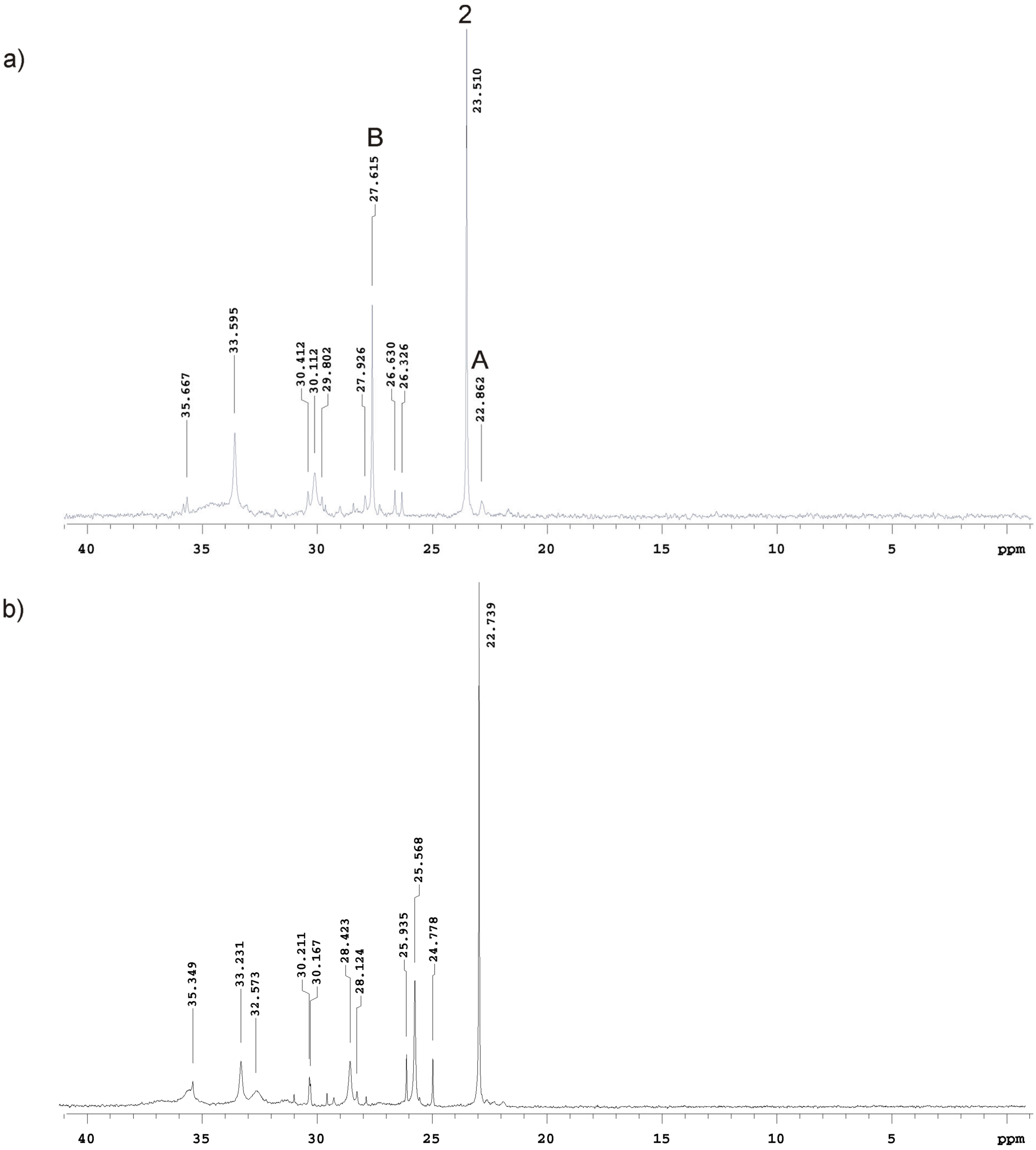

Fig. S15 ^{31}P NMR spectra of the brownish thermolysate of **1** in a) CD_2Cl_2 and b) DMSO-d_6.

The ^{31}P NMR spectrum of the brownish thermolysate of **1** shows several signals (Fig. S15), indicating that a complex mixture of phosphorus containing products were obtained.

Based on the work of Lagunas and co-workers[2] we can assign several signals to Au(I)-xantphos complexes. Thus, the signal at 23.5 ppm corresponds to complex **2**, and signals at 22.9 and 27.7 ppm are from AuCl(L) and $[(AuCl)_2(L)_2]$ complexes in the ^{31}P NMR spectrum (Fig. 15a). Since thermolysis of **1** gives a mixture of products, there are other phosphorous-containing species in CD_2Cl_2 solution. The signal at 22.7 ppm in the ^{31}P NMR spectrum recorded in DMSO-d_6 (Fig. 15b) indicate the presence of AuCl(L).[2]

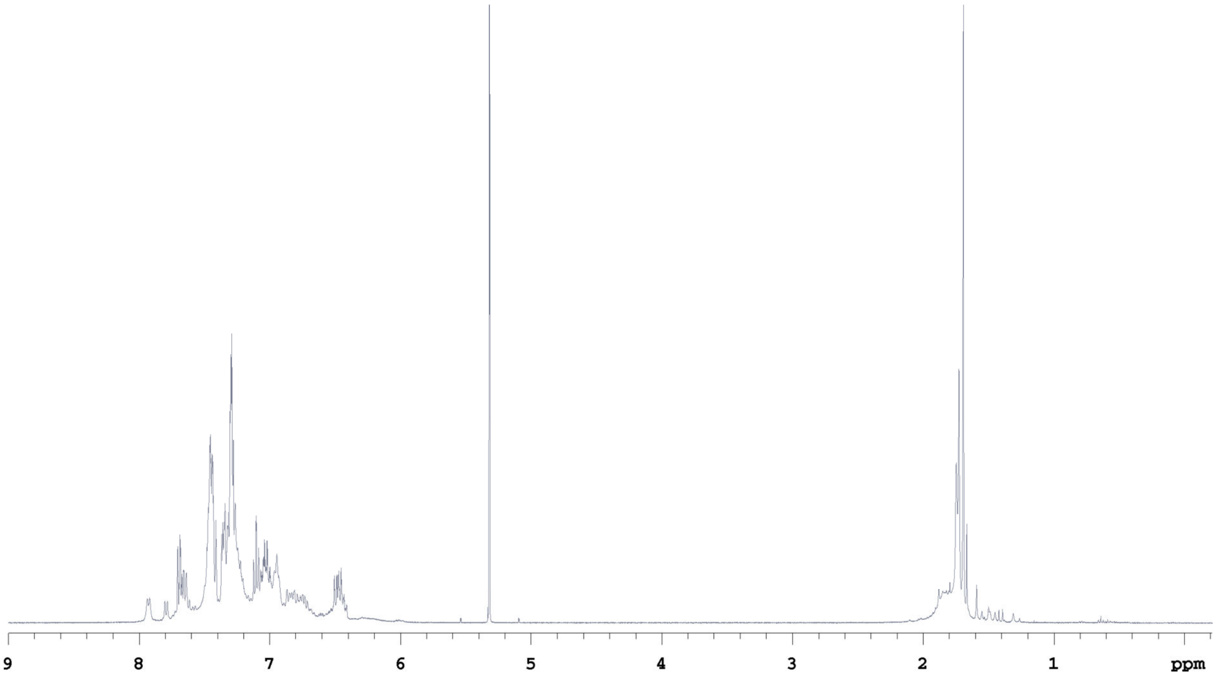

Fig. S16 ^{1}H NMR spectra of the brownish thermolysate of **1** in CD_2Cl_2.

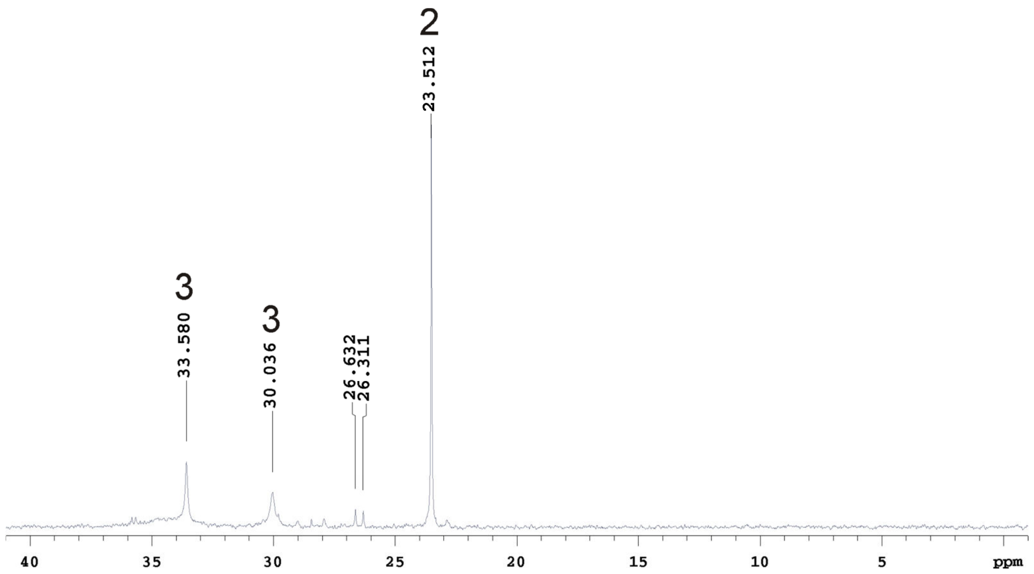

Fig. S17 ^{31}P NMR spectra of the crystals of **2** and **3** in CD_2Cl_2.

We tentatively assign the signals at 33.6 and 30.0 ppm in the ^{31}P NMR spectrum (Fig. S17) to complex **3**. This assignment is in agreement with the ^{31}P chemical shifts reported for $[Au_3(dppm)_2Cl_2]Cl$ (dppm = $Ph_2PCH_2PPh_2$).[3] However, other signals at 26.6 and 26.3 ppm indicate the presence of small amounts of other species.

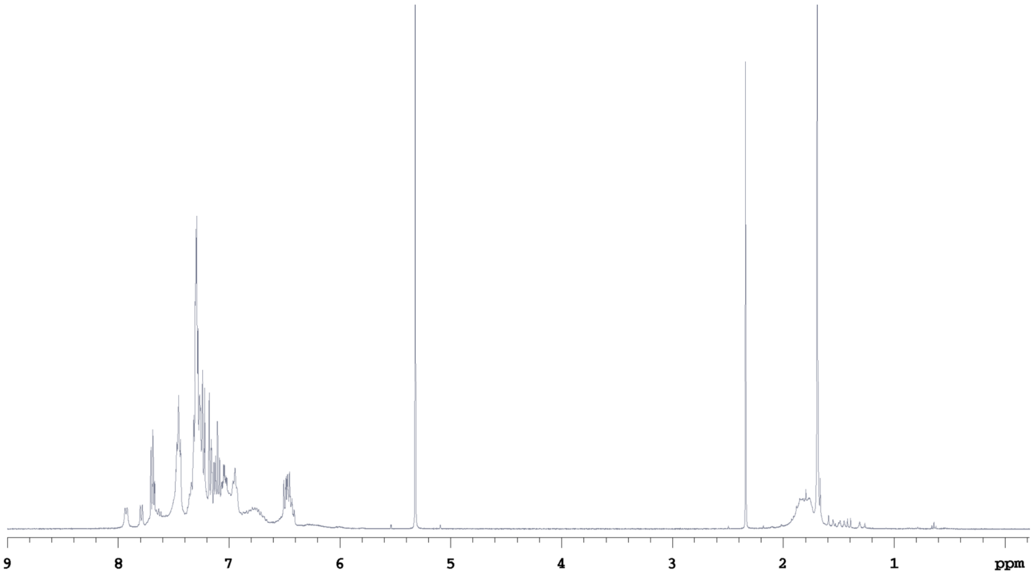

Fig. S18 ^{1}H NMR spectra of the crystals of **2** and **3** in CD_2Cl_2.

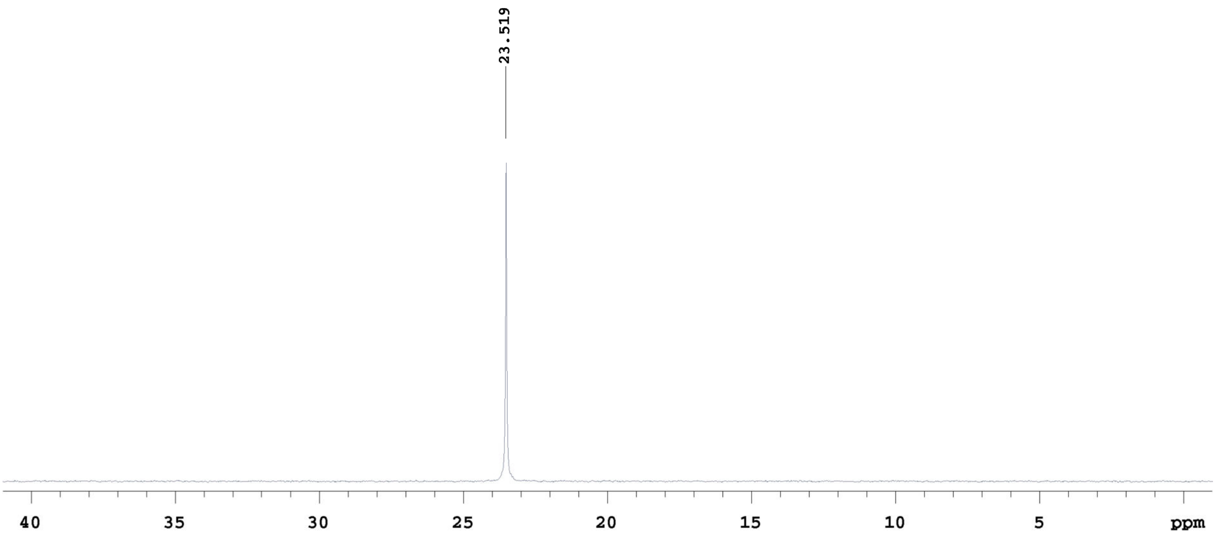

Fig. S19 ^{31}P NMR spectra of crystals of **2** in CD_2Cl_2.

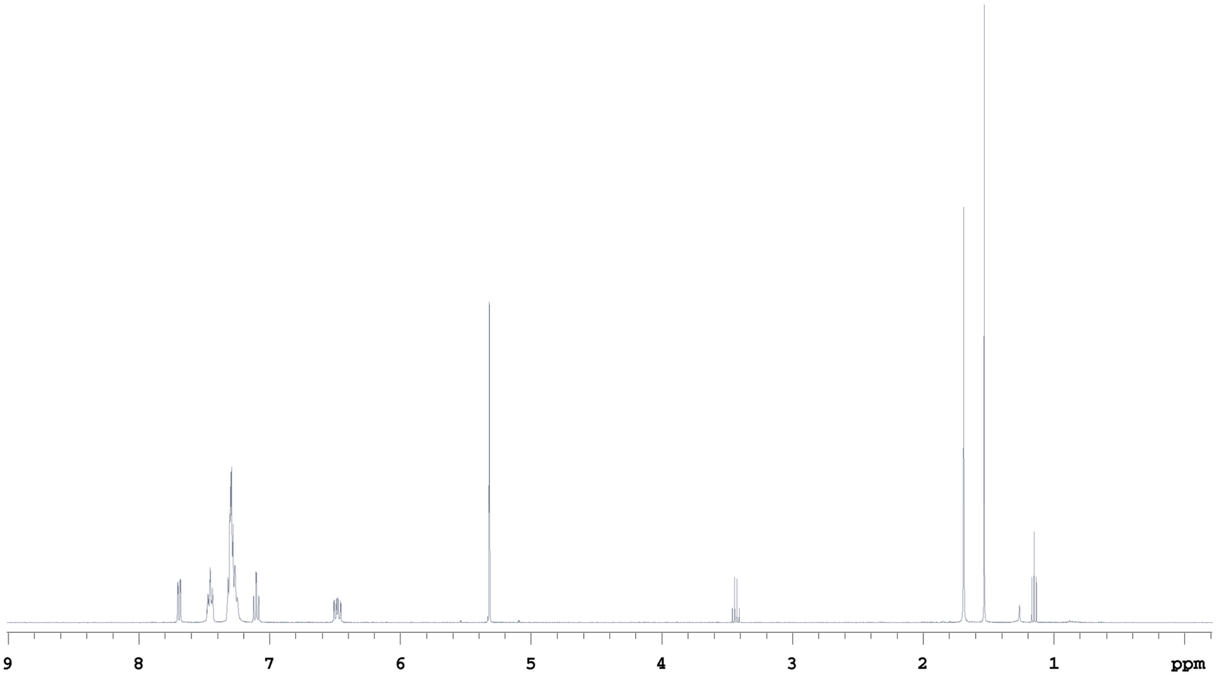

Fig. S20 ^{1}H NMR spectra of crystals of **2** in CD_2Cl_2.

The NMR data of complex **2** has been previously reported.[2]

Single Crystal X-ray Diffraction

Crystals of **2** and **3** were mounted in Paratone-N oil within a conventional cryo-loop, and intensity data were collected on a Rigaku R-AXIS RAPID image plate diffractometer (λ(Mo-K_α radiation) = 0.71075 Å), fitted with an X-stream low temperature attachment. Several scans in the φ and ω direction were made to increase the number of redundant reflections, which were averaged over the refinement cycles. The structures were solved by direct method (*SIR*92)[4] and refined by full-matrix least-squares (*SHELXL*-2014).[5] All non-hydrogen atoms were refined anisotropically in F^2 mode. Hydrogen atomic positions were generated from assumed geometries. The riding model was applied for the hydrogen atoms. Only the methyl hydrogen atoms were refined as riding and rotating groups.

In **2**, the toluene share a site with dichloromethane molecules with an occupancy of 0.80:0.20. The corresponding atoms of the disordered dichloromethane were refined isotropically.

Crystals of **3** diffracted weakly and the solvent of crystallization was easily lost to the atmosphere. As a consequence, there is a large 1076 Å^3 void per unit cell (25.5% volume of the unit cell, Fig. S21), which is filled with disordered solvent molecules, which were not sufficiently resolved in the electron-density map to be modelled with disordered atoms. The contribution of these badly disordered solvent molecules was subtracted from the diffraction data by applying the SQUEEZE procedure in PLATON.[6] SQUEEZE estimated the electron counts in the channels to be 290.

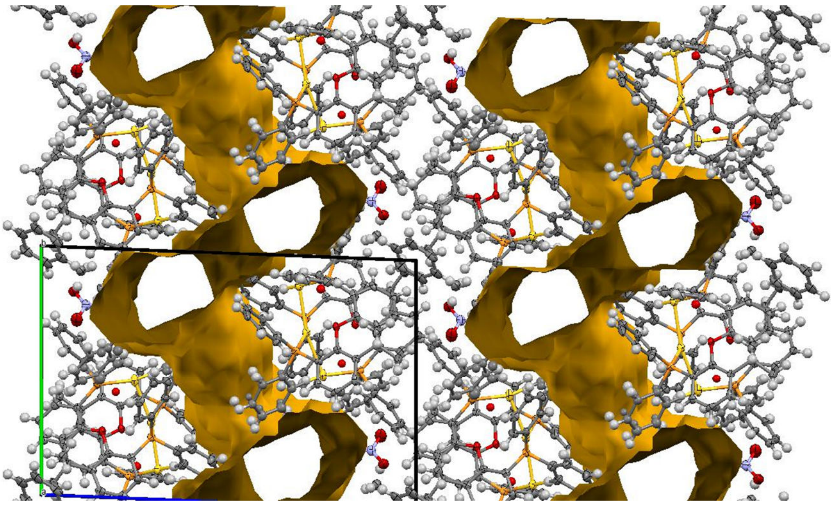

Fig. S21 Packing arrangement showing the large voids viewed along the crystallographic *a* axis in **3**.

The the partial site occupancy of Au(1) and Au(3), and the nearest remaining electron density indicated the presence of P=O bonds. Refinement of the Au:O ratio gives values of 0.60:0.40 for Au(1):O(1P) and 0.87:0.13 for Au(3):O(1P'), respectively. The lower occupancy positions for O(1P') and O(1P) atoms were refined with isotropic displacement parameters. The C34'–C39' and C22A–C27A phenyl rings are positionally disordered over two sites with an occupancy of 0.60:0.40. The two positions were refined with isotropic displacement parameters.

As shown in Figure S22, the crystal structure of **3** contains $[Au_3(L')_2]^+$ (major component) and two independent $[Au_2(L')(LO)]^+$ cations (minor components). As was shown by the MS ESI, both $[Au_3(L')_2]^+$ and $[Au_2(L')(LO)]^+$ were present in the thermolysate of **1**, thus they can crystallize together to form the mixed crystal of **3**. The HR-MS ESI spectrum (Fig. S23) of a crystal of **3** revealed a peak at 1565.61 *m*/*z*, consistent with formation of $[Au_2(L')(LO)]^+$.

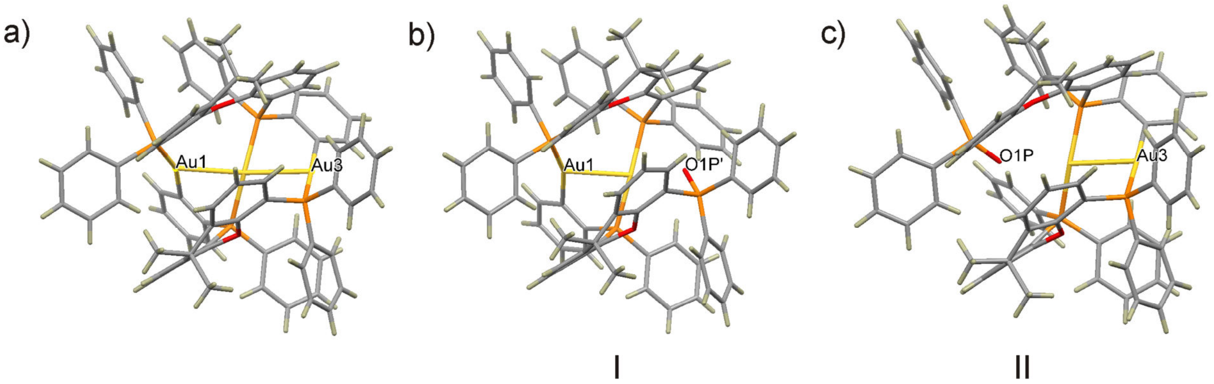

Fig. S22 Molecular structure of a) $[Au_3(L')_2]^+$ (major component) and b)–c) $[Au_2(L')(LO)]^+$ cations (minor components I and II) in the crystal structure of **3**.

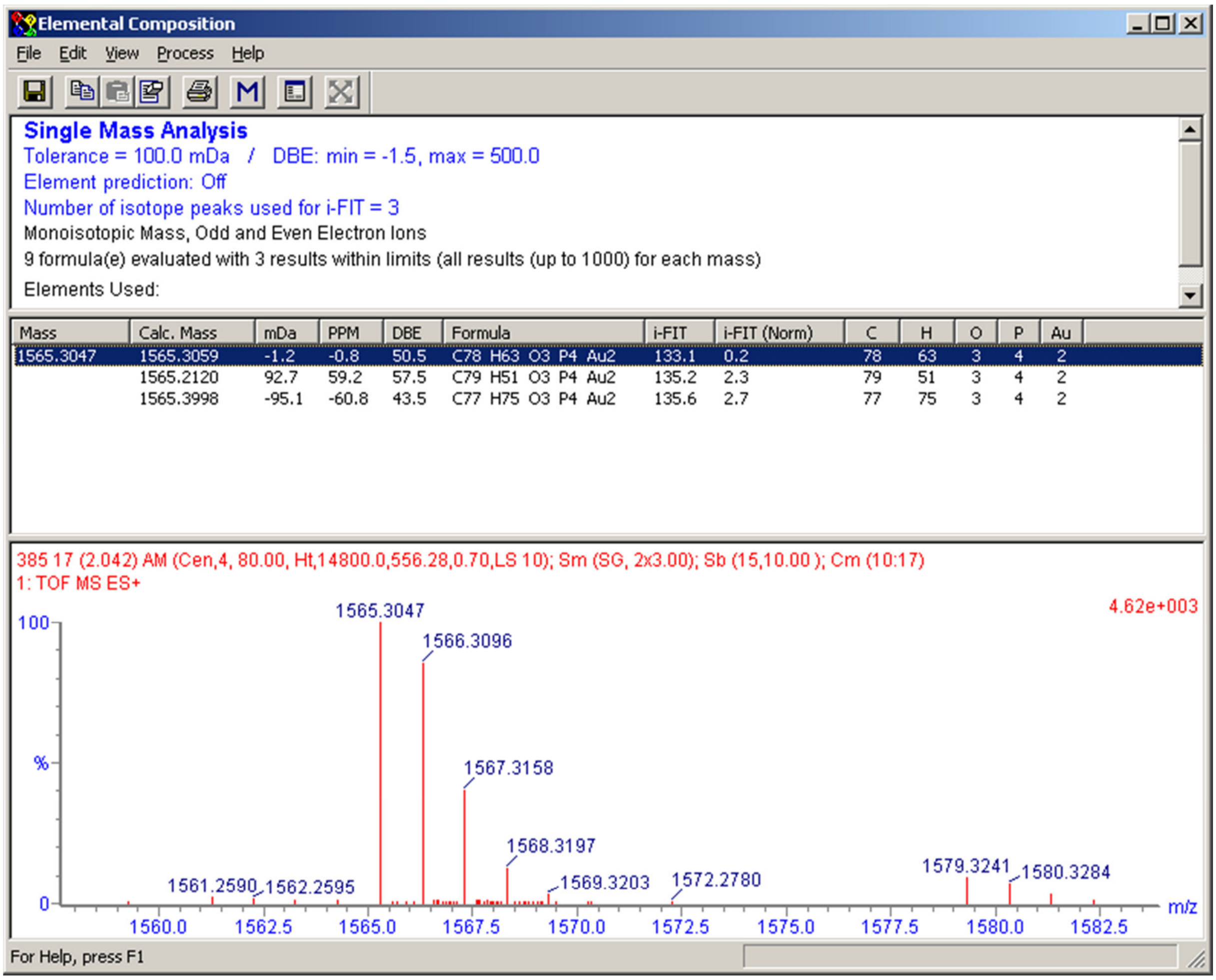

Single Mass Analysis
Tolerance = 100.0 mDa / DBE: min = -1.5, max = 500.0
Element prediction: Off
Number of isotope peaks used for i-FIT = 3
Monoisotopic Mass, Odd and Even Electron Ions
9 formula(e) evaluated with 3 results within limits (all results (up to 1000) for each mass)
Elements Used:

Mass	Calc. Mass	mDa	PPM	DBE	Formula	i-FIT	i-FIT (Norm)	C	H	O	P	Au
1565.3047	1565.3059	-1.2	-0.8	50.5	C78 H63 O3 P4 Au2	133.1	0.2	78	63	3	4	2
	1565.2120	92.7	59.2	57.5	C79 H51 O3 P4 Au2	135.2	2.3	79	51	3	4	2
	1565.3998	-95.1	-60.8	43.5	C77 H75 O3 P4 Au2	135.6	2.7	77	75	3	4	2

385 17 (2.042) AM (Cen,4, 80.00, Ht,14800.0,556.28,0.70,LS 10); Sm (SG, 2x3.00); Sb (15,10.00); Cm (10:17)
1: TOF MS ES+

Fig. S23 HRMS-ESI spectra of $[Au_2(L')(LO)]^+$.

Crystal data, data collection and refinement details for **2** and **3** are listed in Table S1.

Table S1 Crystal data and structure refinement parameters for **2** and **3**, respectively.

Complex	**2**	**3**
Formula	$C_{39}H_{32}Au_2O_1P_2Cl_2$ 0.8 (C_7H_8), 0.2 (CH_2Cl_2)	$C_{78}H_{62.53}Au_{2.47}O_{2.53}P_4$, NO_3, 0.5 (C_7H_8)
Formula weight	1134.11	3517.50
Crystal size [mm]	0.83 × 0.75 × 0.29	0.25 × 0.25 × 0.05
Colour	colourless	colourless
Crystal system	monoclinic	triclinic
Space group	$P2_1/n$	$P\bar{1}$
Temp. (K)	108(2)	103(2)
a [Å]	12.1273(9)	12.6109(18)
b [Å]	21.3275(13)	15.351(2)
c [Å]	15.5941(11)	22.690(3)
α [°]	90	90.421(3)
β [°]	101.076(2)	97.725(3)
γ [°]	90	103.650(3)
V [Å^3]	3958.2(5)	4226.2(10)
Z	4	2
d_{calc} [Mg/m^3]	1.903	1.383
μ [mm^{-1}]	7.682	4.400
F(000)	2178	1724
No. of collected reflns.	72810	133257
No. of indep. reflns./R_{int}	9806/0.091	15413/0.104
No. of obsd. reflns. $I > 2\sigma(I)$	8833	6877
No. of parameters	486	778
GOF	1.08	0.86
$R1$ (obsd. data)	0.0483	0.0679
$wR2$ (obsd. data)	0.1080	0.1446
Largest diff. peak/ hole (e Å^{-3})	2.17/–1.98	3.06/–4.08

Computational studies

In the present study density functional theory (DFT) and time-dependent density functional theory (TD DFT) calculations were performed by using the *Gaussian 09* program package[7] at the PBE0/6-31G* level of theory.[8] Relativistic effects were included for the Au atom by using the Los Alamos National Laboratory double zeta type (LANL2DZ) pseudopotential.

To interpret the spectroscopic properties of components of **3**, preliminary TD DFT calculations were effectuated for the lowest energy singlet states (S_1) of crystalline structures of $[Au_3(L')_2]^+$ and $[Au_2(L')(LO')]^+$ cations fixed in their X-ray geometries. The results of these calculations (Table S2) showed that only the trinuclear $[Au_3(L')_2]^+$ cation can be excited with 365 nm UV light, so the more time consuming optimization steps and emission analysis were performed only for the $[Au_3(L')_2]^+$ cation.

The geometries of the singlet ground state (S_0) and triplet excited state (T_1) of the $[Au_3(L')_2]^+$ cation were fully optimized in the gas phase without symmetry constraints. Due to convergence problems with the TD DFT optimization, the structure for the lowest triplet excited states (T_1) of the complex cation was optimized with the unrestricted UPBE0/LANL2DZ method. After geometry optimization the excited states were investigated by TD DFT analysis. The absorption energies were obtained by TD DFT method at the optimized ground state geometry using the same functional and basis sets as for geometry optimization. The lowest energy triplet emission was determined by TD DFT calculation with PBE0 functional at the optimized triplet (T_1) structure. The molecular orbital surfaces were plotted by Molekel 5.4 visualization software at an isosurface value of 0.03 au.[9]

Table S2 Absorption wavelengths (λ), oscillator strengths (f) and orbital compositions for the lowest energy singlet excited states (S_1) of $[Au_3(L')_2]^+$ and $[Au_2(L')(LO')]^+$ cations computed by TD DFT method (H = HOMO, L = LUMO) *based on X-ray diffraction geometries*.

Components	λ (nm)	f	Assignment
$[Au_3(L')_2]^+$	356.5	0.1166	H→L (85%), H→L+2 (6%)
$[Au_2(L')(LO')]^+$ (I)	321.9	0.1004	H→L+1 (61%), H→L+2 (22%), H→L (8%)
$[Au_2(L')(LO')]^+$ (II)	324.8	0.0580	H→L+1 (82%), H→L+2 (13%)

Table S3 Selected bond lengths (Å), bond angles (°) and torsion angles (°) in *optimized* singlet ground state (S_0) and triplet excited state (T_1) structures of $[Au_3(L')_2]^+$ cation.

	S_0	**T_1**
Au(1)−P(1)	2.372	2.396
Au(3)−P(1')	2.371	2.397
Au(2)−P(2)	2.345	2.546
Au(2)−P(2')	2.346	2.541
Au(1)−C(35')	2.051	2.044
Au(3)−C(35)	2.051	2.044
Au(1)···Au(2)	3.012	2.696
Au(2)···Au(3)	3.011	2.699
P(1)–Au(1)−C(35')	169.0	167.6
P(1')–Au(3)−C(35)	169.1	168.1
P(2)–Au(2)−P(2')	165.0	152.5
Au(1)···Au(2)···Au(3)	168.7	177.7
P(1)–Au(1)···Au(2)–P(2)	57.4	68.2
P(1')–Au(3)···Au(2)–P(2')	57.9	68.5

Table S4 Absorption and emission wavelengths (**λ**), oscillator strengths (***f***) and orbital compositions for *optimized structure* of $[Au_3(L')_2]^+$ cation computed by TD DFT method (H = HOMO, L = LUMO).

Excited state	λ(nm)	f	Assignment
S_1	327.6	0.0245	H→L+1 (88%), H→L+4 (6%)
S_2	**326.4**	**0.1928**	**H→L (95%)**
S_3	311.7	0.0022	H→L+3 (40%), H→L+4 (44%), H→L+1 (4%), H→L+6 (5%), H→L+9 (3%)
S_4	302.1	0.0122	H→L+2 (95%)
S_5	298.8	0.0002	H→L+3 (55%), H→L+4 (33%), H→L+1 (3%), H→L+6 (4%)
S_6	290.7	0.0000	H-1→L+1 (26%), H→L+2 (28%), H→L+3 (30%), H-2→L (3%), H→L (3%)
S_7	290.1	0.0195	H→L+5 (94%)
S_8	287.6	0.0080	H→L+8 (71%), H→L+10 (21%)
S_9	285.5	0.0007	H→L+6 (80%), H→L+4 (8%), H→L+7 (2%)
S_{10}	280.4	0.0157	H-2→L+1 (12%), H-1→L (46%), H-1→L+1 (13%), H-2→L (5%), H→L+9 (4%)
S_{11}	280.2	0.0295	H-2→L (21%), H-1→L (13%), H-1→L+1 (39%), H-2→L+1 (4%), H→L+10 (2%)
S_{12}	278.2	0.0014	H→L+9 (68%), H-1→L (8%), H→L+7 (3%), H→L+11 (4%), H→L+14 (3%)
S_{13}	276.9	0.0023	H-3→L (11%), H-2→L+1 (45%), H-1→L (10%), H-1→L+2 (15%), H-3→L+2 (3%), H-2→L+3 (4%)
S_{14}	276.5	0.0003	H→L+8 (23%), H→L+10 (56%), H-1→L+1 (7%), H→L+13 (4%)
S_{15}	275.0	0.0227	H-4→L (11%), H-3→L+1 (13%), H-2→L (37%), H-1→L+1 (19%), H→L+10 (3%)
S_{16}	**272.2**	**0.1543**	H-3→L+1 (12%), **H-2→L+2 (40%)**, H-1→L+3 (14%), H-4→L (5%), H-2→L (4%), H-1→L+4 (7%), H→L+10 (4%)
S_{17}	271.3	0.0010	H-3→L (51%), H-2→L+3 (12%), H-1→L+2 (12%), H-4→L+1 (4%), H-3→L+2 (4%), H-2→L+4 (5%)
S_{18}	270.4	0.0025	H→L+11 (14%), H→L+12 (34%), H→L+13 (31%), H→L+10 (4%)
S_{19}	269.4	0.0003	H→L+9 (10%), H→L+11 (55%), H→L+12 (16%), H→L+6 (3%), H→L+14 (5%)
S_{20}	266.1	0.0013	H-2→L+1 (14%), H-4→L (6%), H-4→L+1 (8%), H-3→L (9%), H-2→L (5%), H-2→L+3 (5%), H-1→L (9%), H-1→L+2 (9%)
T_1	**582.6**	**0.0000**	**H→L (98%)**

Table S5 Compositions of the dominant molecular orbitals involved in the main absorption and emission transitions for *optimized structure* of $[Au_3(L')_2]^+$ cation obtained from TD DFT analysis.

Transition	λ(nm)	Orbital	Au atoms[a]			Phosphine ligands
			s	p	d	
$S_0 \rightarrow S_2$	326.4	HOMO	0.124	0.014	0.252	0.381
			0.055	0.000	0.174	
		LUMO	0.002	0.139	0.008	0.794
			0.000	0.055	0.003	
$S_0 \rightarrow S_{16}$	272.2	HOMO–2	0.000	0.006	0.005	0.985
			0.000	0.001	0.002	
		LUMO+2	0.013	0.06	0.004	0.921
			0.000	0.001	0.000	
$T_1 \rightarrow S_0$	582.6	HOMO	0.089	0.033	0.220	0.435
			0.020	0.000	0.203	
		LUMO	0.000	0.106	0.016	0.541
			0.208	0.056	0.074	

[a] The first and second lines correspond to the terminal and the middle Au atoms respectively.

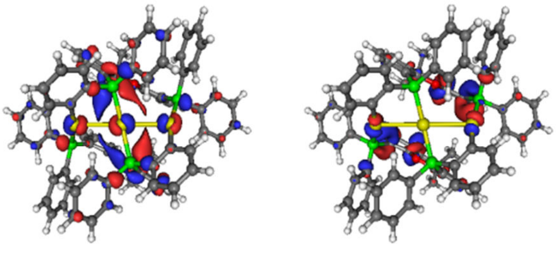

LUMO LUMO + 2

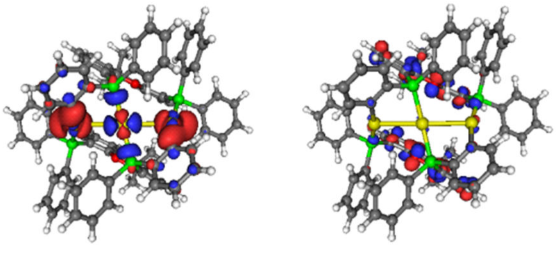

HOMO HOMO – 2

Fig. S24 Molecular orbital surfaces related to the ground state of $[Au_3(L')_2]^+$ cation.

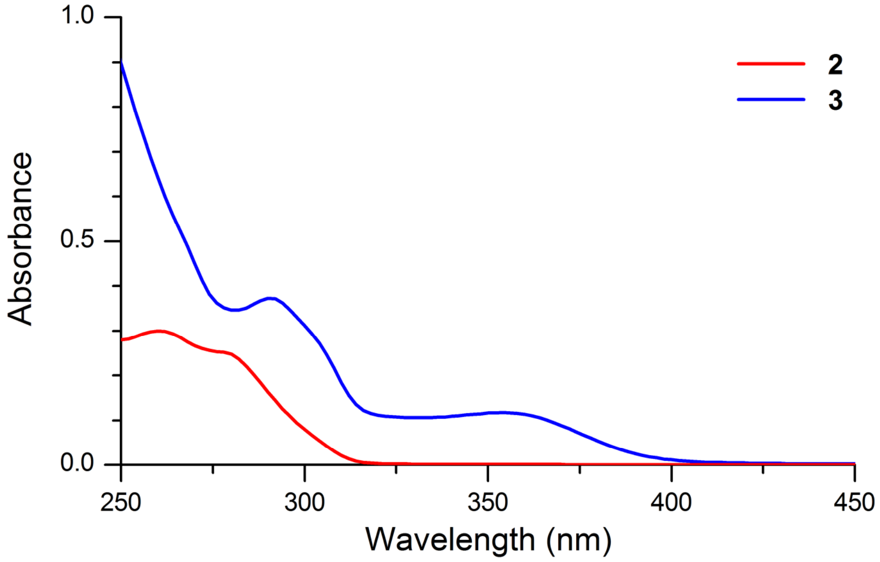

Fig. S25 UV/VIS absorption spectra of **2** and **3** in CH_2Cl_2 at concentration of 10 μM.

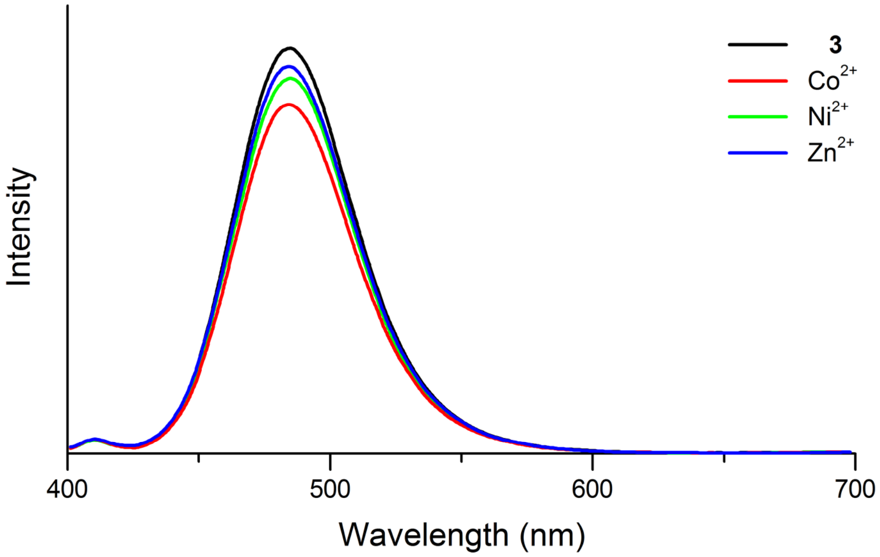

Fig. S26 Emission spectra of **3** in methanol (10 μM) with different metal cations at concentration of 10^{-3} M.

Acknowledgements

The authors gratefully acknowledge the support by MTA (Hungarian Academy of Sciences) through the Lendület Programme (LP2012-21/2012).

The authors are indebted to Dr. Zsuzsanna Czégény (Environmental Chemistry Research Group, Institute of Materials and Environmental Chemistry, Research Centre for Natural Sciences, Hungarian Academy of Sciences, Budapest, Hungary) for Pyrolysis–gas chromatography/mass spectrometry (Py–GC/MS) measurements. We also thank Dr. Ágnes Gömöry and Dr. Olivér Ozohanics (MS Proteomics Research Group, Institute of Organic Chemistry, Research Centre for Natural Sciences, Hungarian Academy of Sciences, Budapest, Hungary) for HRMS-ESI measurements. The authors are indebted to Dr. Attila Domján (NMR Spectroscopy Research Group, Institute of Organic Chemistry, Research Centre for Natural Sciences, Hungarian Academy of Sciences, Budapest, Hungary) for NMR spectroscopy measurements.

References

1. Cs. Jobbágy, M. Molnár, P. Baranyai, A. Hamza, G. Pálinkás, A. Deák, *CrystEngComm,* 2014, **16**, 3192–3202.
2. A. Pintado-Alba, H. de la Riva, M. Nieuwhuyzen, D. Bautista, P. R. Raithby, H. A. Sparkes, S. J. Teat, J. M. López-de-Luzuriaga and M. C. Lagunas, *Dalton Trans.*, **2004**, 3459–3467.
3. I. J. B. Lin, J. M. Hwang, D.-F. Feng, M. C. Cheng, Y. Wang, *Inorg. Chem,* 1994, **33**, 3467–3472.
4. A. Altomare, G. Cascarano, C. Giacovazzo, A. Guagliardi, M. C. Burla, G. Polidori, M. Camalli, *J. Appl. Cryst.*, 1994, **27**, 435.
5. G. M. Sheldrick, *Acta Cryst.*, 2015, **C71**, 3–8.
6. a) A. L. Spek, *PLATON*, A Multipurpose Crystallographic Tool, Utrecht University, Utrecht, The Netherlands, 2008; b) A. L. Spek, *J. Appl. Cryst.*, 2003, **36**, 7–13.
7. *Gaussian 09*, Revision C.01, M. J. Frisch, G. W. Trucks, H. B. Schlegel, G. E. Scuseria, M. A. Robb, J. R. Cheeseman, G. Scalmani, V. Barone, B. Mennucci, G. A. Petersson, H. Nakatsuji, M. Caricato, X. Li, H. P. Hratchian, A. F. Izmaylov, J. Bloino, G. Zheng, J. L. Sonnenberg, M. Hada, M. Ehara, K. Toyota, R. Fukuda, J. Hasegawa, M. Ishida, T. Nakajima, Y. Honda, O. Kitao, H. Nakai, T. Vreven, J. A. Montgomery, Jr., J. E. Peralta, F. Ogliaro, M. Bearpark, J. J. Heyd, E. Brothers, K. N. Kudin, V. N. Staroverov, R. Kobayashi, J. Normand, K. Raghavachari, A. Rendell, J. C. Burant, S. S. Iyengar, J. Tomasi, M. Cossi, N. Rega, J. M. Millam, M. Klene, J. E. Knox, J. B. Cross, V. Bakken, C. Adamo, J. Jaramillo, R. Gomperts, R. E. Stratmann, O. Yazyev, A. J. Austin, R. Cammi, C. Pomelli, J. W. Ochterski, R. L. Martin, K. Morokuma, V. G. Zakrzewski, G. A. Voth, P. Salvador, J. J. Dannenberg, S. Dapprich, A. D. Daniels, Ö. Farkas, J. B. Foresman, J. V. Ortiz, J. Cioslowski, and D. J. Fox, *Gaussian*, Inc., Wallingford CT, 2009.
8. Y. Zhao and D. G. Truhlar, *Acc. Chem. Res.*, 2008, **41**, 157–167.
9. Ugo Varetto, Molekel 5.4, http://ugovaretto.github.io/molekel/